We are IntechOpen, the world's leading publisher of Open Access books
Built by scientists, for scientists

6,900
Open access books available

185,000
International authors and editors

200M
Downloads

154
Countries delivered to

Our authors are among the

TOP 1%
most cited scientists

12.2%
Contributors from top 500 universities

BOOK CITATION INDEX
CLARIVATE ANALYTICS
INDEXED

WEB OF SCIENCE™

Selection of our books indexed in the Book Citation Index
in Web of Science™ Core Collection (BKCI)

Interested in publishing with us?
Contact book.department@intechopen.com

Chapter

Synthesis Process Optimization of Polyimide Nanocomposite Multilayer Films, Their Dielectric Properties, and Modeling

Shakeel Akram, Jérôme Castellon, Serge Agnel and Jean-Pierre Habas

Abstract

Polymer nanocomposite-based dielectric materials are playing a vital role in the area of electrical insulation research and developments. The nanoparticle dispersion and interface region are the crucial parts of these developments. This chapter begins with the description of physical properties and their derived nanoparticles of polyimide (PI) films. Then, the detailed synthesis process of PI/nanocomposite multilayer film and its optimization is discussed in this chapter. Several factors in the synthesis process, which can influence the quality of the film, are discussed. After synthesis, the dielectric properties such as space charge were measured, and the results are compared with single and multilayer PI/nanocomposite films. Simulations and modeling help to shed light on the experimental results and create an understanding of polymer nanocomposite properties. Therefore, the PI/nanocomposite multilayer 3D model based on boundary conditions obtained from SEM/TEM images of synthesized samples was also constructed and simulated in COMSOL multiphysics software. The nanoparticle agglomeration and the impact of nanoparticle dispersion on the electrical properties of the material are described in detail in this model. The results demonstrate that the nanoparticle dispersion is improved by using a thin layer of PI/nanocomposite on PI film. As a result, fewer space charges and low electric fields are observed in multilayer films.

Keywords: polyimide nanocomposite, multilayer insulation, synthesis optimization, dielectric properties, polyimide nanocomposite modeling

1. Introduction

Electrical insulations are the key components for electric motors, which are used in space crafts and electric trains. Polyimide (PI) films as an insulating material are used in such motors, which are commercially available in single- and multicoated forms. Over the past few years, global market has shown a great interest in the application of nanodielectrics, especially in the field of electrical insulating materials. Various research results have claimed that polymer nanocomposite materials can improve dielectric properties for electrical insulation applications [1–4]. The key role played by the nanoparticle dispersion and interface region are essential

parts of these improvements. Further conditions to advances are the size and type of nanoparticles properly chosen and distributed into the polymer matrix. Initially, it seemed like magic that everything is possible by using nanodielectrics, which later proved wrong after understanding the exact working principles of polymer-based nanocomposites, though several questions still need to be solved [5]. This has motivated the author to explore in this field further and find those principles by using experimental and simulation work on improving the dielectric properties of polyimide-based nanocomposite.

This chapter begins with a description of the physical properties of polyimide and its derived nanoparticles. Afterward, a detailed synthesis process of polyimide nanocomposite single and multilayer films is outlined leading to the synthesis process optimization. Polyimide nanocomposites are the leading component in the advancement of electric motors and generator's insulating materials. However, nanoparticle dispersion is the primary concern to improve polymer nanocomposite dielectric properties. In this work, polyimide-based nanocomposite single- and multilayer films are synthesized and characterized in detail. The preparation of polyimide nanocomposite is a complex process with many variables involved. Therefore, it is vital to know the right chemistry when dealing with it. Several methods were probed before an optimal synthesis process was found. A detailed synthesis process optimization is described at the end of this chapter to understand all variables that can alter the dielectric properties of the polyimide nanocomposite films.

1.1 Polyimide insulation films and their physical properties

Thermo-oxidative polyimide films by DuPont are in the market since the 1960s. These low dielectric constant thin films are highly corona resistive, are thermally stable, and have higher breakdown strength electrically and mechanically [6]. Such unique characteristics have made polyimide films to use in large industrial applications such as aerospace, automotive, and microelectronic devices. The fire resistance property of PI and low dielectric constant has made it possible to isolate metal lines and reduce electromagnetic interference effect in electronics and signal processing devices [6]. Polyimide is also used in electric motor insulation for high-speed trains. Polyimide is a high-temperature organic class of polymer that is mechanically robust and thermally stable based on stiff aromatic backbones [6]. The main functional groups in polyimide structure are aromatic ring, amide, and ether groups. There are several monomers and methods available to synthesize the polyimide. Therefore, a slight change in the monomer's structure and synthesis process can alter the physical properties of PI films significantly. Polyimides are chemically closed structure polymers that are nonreactive to many chemicals such as solvents and oils. Polyimides are intrinsically resistive to heat and flame retardants. PI is also resistive to acids but avoids to use in alkalis and inorganic acid environment. The remarkable radiation resistant property of PI has made it an ideal material to use in outer space radiation environment and in nuclear reactors, where PI is used alone as well as in composite forms. The changes in the dimension of material per 1°C rise in temperature are called the coefficient of thermal expansion. PI exhibits higher values of thermal expansion coefficient than other polymers. PI undergoes numerous phase changes to 400°C during the imidization process from polyamic acid solution to thin solid films. PI is a thermally stable polymer that has a very high value of T_g and only 5% weight loss above 400°C [6]. Therefore, it is a very suitable material for packaging applications. PI films have higher mechanical strengths. The stress-strain results have sown that the flawless PI films have mechanical strength in between 100 and 200 MPa and the elongation at break in between 10 and 25% [6]. The mechanical vibrations in electric motors and metal conductor's contact in electronic packaging applications can cause severe damage to

the mechanical strength of PI films. If the films are brittle and the applied force due to mechanical vibrations crosses the fracture limit, then the internal cracks or defects can break the insulation. The brittleness of PI films can be controlled during the synthesis process by using different monomers and imidization temperature and time [6]. The physical properties of polyimide films at room temperature are shown in **Table 1**.

1.2 Properties of polyimide in electrical engineering

1.2.1 Dielectric constant and dielectric loss

When the dielectric material is subjected to an electric field, it becomes polarized due to the movement of induced and permanent electric dipoles [7]. For ideal insulation, the movement of dipoles should be zero or very low to block the conduction current. The value of dielectric constant (ε') defines the polarization ability of dielectric material. The movement of dipoles in an alternating electric field causes the loss of energy known as a dielectric loss (ε''). The conduction loss and dielectric loss are two significant losses that are responsible for energy loss in a dielectric material. The movement of charges determines the conduction loss, while the movement of dipoles determines the dielectric loss, the movement of dipoles causes the energy dissipation as the polarization switches its direction in an alternating electric field. The polarization lags the alternate electric field to produce heat, and dielectric loss increases at the relaxation frequencies. Therefore, the value of dielectric constant reduces quickly at relaxation frequencies because the polarization is not able to keep pace with the alternating electric field, as illustrated in **Figure 1**. An efficient insulating dielectric material blocks the conduction with a minimum dissipation of energy. The materials with a higher value of dielectric constant usually have a higher dielectric loss. The energy loss in dielectrics can be used to heat the food in a microwave oven. The orientational polarization in water frequency is utilized for this process, which is close to the relaxation or resonance frequency. It means water molecules absorb a lot of energy, which later dissipated to heat the food. The dielectric constant of polyimide films varies from 3.0 to 3.8 according to the structure and composite fillers added into it [7].

The relative permittivity is composed of two parts: the real part denoted as ε' and the imaginary part indicated as ε''. The ratio of these two values is defined as the dissipation factor and given as follows:

$$\tan\delta = \frac{\varepsilon''}{\varepsilon'} \tag{1}$$

| Properties	Typical value at 25°C	Test methods
Tensile strength, MPa	231	ASTM D-882-91
Density, g/cc or g/mL	1.42	ASTM D-1505
Glass transition temperature (T$_g$), °C	360–410	Differential calorimetry
Thermal conductivity, W/m.K	0.12	ASTM F-433
Electrical breakdown strength, kV/mm	280	ASTM D-149
Dielectric constant at 1 kHz	3.4	ASTM D-150
Dissipation factor at 1 kHz	0.0020	ASTM D-150
Volume resistivity, Ω.cm	1.5E17	ASTM D-257

Table 1.
Properties of polyimide.
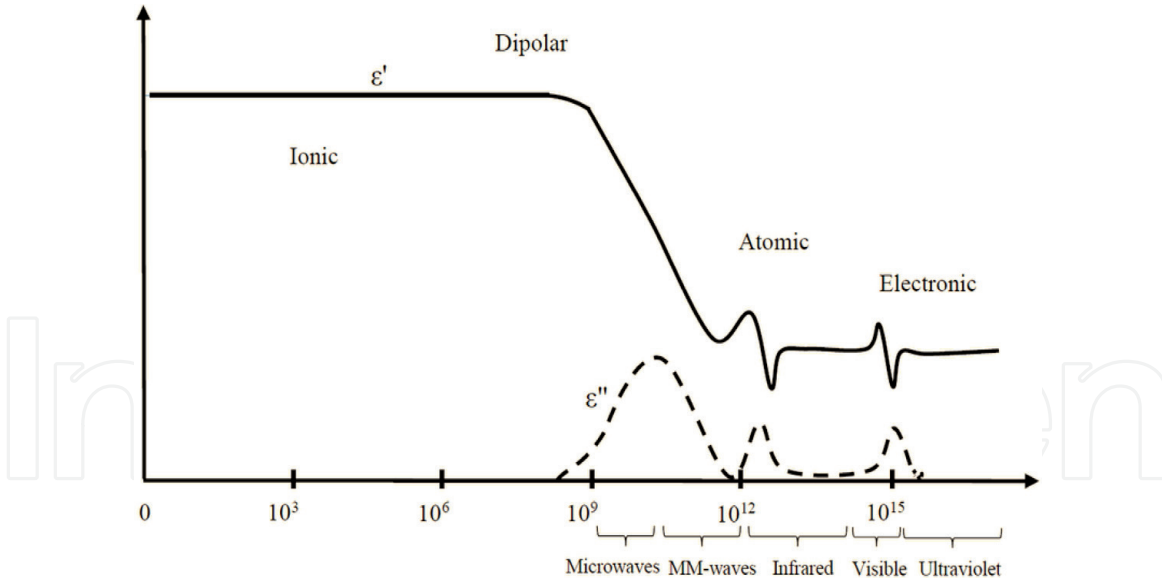
Figure 1.
Dielectric loss vs. frequency.

Typically, PI films have dissipation loss in between 0.001 and 0.02 [8]. The low tan δ value indicates that PI loses less electrical energy. The low dielectric constant and low dielectric loss make PI films suitable to use in electrical signal packaging applications to avoid signal interference.

1.2.2 Conduction current

Conduction current attributes to different polarization and depolarization processes happening inside the material. The complete polarization process can be presented as Eq. (2) [9].

$$i_p = i_i + i_a + i_c \tag{2}$$

where i_i is the instantaneous current due to the displacement polarization, i_a represents the relaxation polarization current, and i_c presents the conduction current due to the conductivity of the specimen. The Simons and Tam theory represents that the depolarization current is a superposition of different relaxation processes depending on the trap levels [9]. There are several polarizations due to dipole relaxation process that may take place in a dielectric material as follows:

1. Electronic polarization

2. Ionic polarization

3. Orientation polarization

4. Interfacial/space charge polarization

5. Hopping polarization

1.2.3 Dielectric breakdown strength

The breakdown strength is the ability of dielectric material to oppose electric field stresses without any insulation breakage or passing a certain amount of leakage current. The value of dielectric breakdown strength can be found as

the applied voltage at which the electric breakdown occurred. The breakdown strength may vary by varying the temperature, moisture, and defects inside the material. The PI films that we synthesized have breakdown strength between 150 and 260 kV/mm [8, 10]. Due to its high electrical breakdown strength and mechanically tough properties, PI as an insulation can be useful to utilize in a high voltage industry applications, where electrical instruments can produce strong electrical field and leakage current to damage the insulation. Dielectric strength can vary due to the following reasons:

1. Nonhomogenous nature of sample thickness

2. Decrease with an increase in temperature

3. Decrease with an increase in frequency

4. Decrease with an increase in humidity

1.2.4 Charge transport phenomena

The PI films can be amorphous or crystalline, depending on their synthesis chemistry. In these regions, the trap energy of electrons varies according to the band structure [11]. The high electric field stresses create more trap levels in the insulation, especially at the top and bottom surface of samples near to the electrodes. These trap levels reduce toward the interior regions. In **Figure 2**, a thin PI film is placed between two electrodes. The layer near to anode can act as hole transport layer, and the layer near to cathode can act as electron transport layer. The intersection region of these layers can provide enough space for the recombination of electrons and holes that are injected by electron
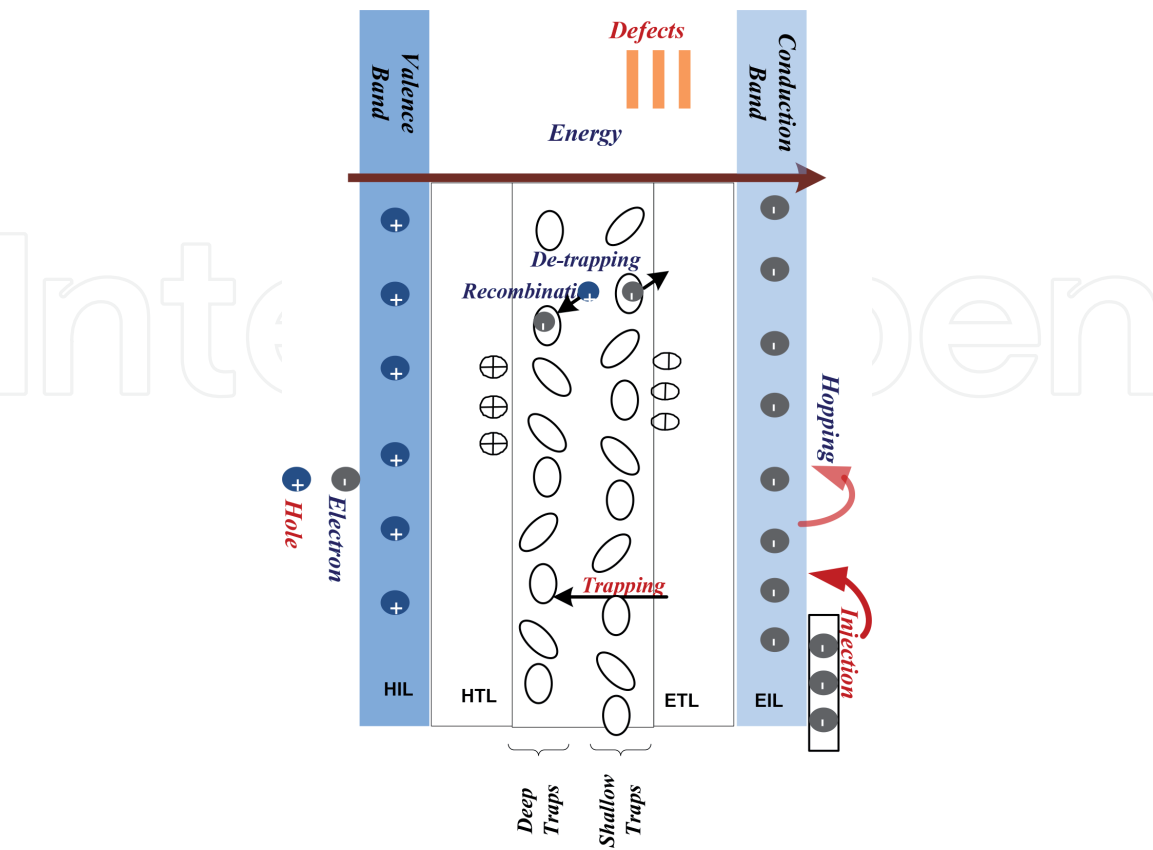

Figure 2.
PI film layer structure, hole injection layer (HIL), hole transport layer (HTL), electron transport layer (ETL), electron injection layer (EIL).

5

injection layer (EIL) and hole injection layer (HIL), respectively. As illustrated in **Figure** 2, the injection of holes from HIL and the injection of electrons from EIL move toward hole transport layer (HTL) and electron transport layer (ETL), respectively.

The charges move from one electrode to the opposite polarity electrode; during the movement, some charges are trapped, some detrapped, and some recombined in the interfacial region due to charges already exist in these regions. The polarity of these interfacial regions depends on the electronic state of the adjacent electrode. In case of PI nanocomposite multilayer structure, the accumulation of charges can depend on the following [10]:

1. The mobility of electrons and holes

2. The distinctive charge barriers at the interface

3. The charge injection rate

4. The polarity of the existing charges at the interface

5. Permittivity and conductivity contrast at interface

Therefore, the discontinuity of electronic state distribution causes an additive trap at the interface for the transportation of charges.

1.2.5 Corona discharge resistance and material degradation

The ionization of air in the form of an electrical discharge is known as corona discharge. This ionization occurs when the electric field crosses the threshold value of air breakdown. Partial or surface discharge is also a kind of corona discharge because it is half discharged to bridge between the electrodes [12]. Corona discharge appears in the form of a lightning color. In high voltage laboratory, corona discharge can be originated using a simple rod to plane electrodes with an air gap between them. Extensive research work has been studied on the appropriate electric field stress to set up corona discharge [12]. Corona discharge depends on the following parameters:

1. Air or gas ionization limit and free path for gas molecules

2. Electrode geometry and surface conditions

3. Distance between the electrodes

4. Insulation structure design flaws

Corona discharges can damage the insulation significantly. With the growing demand for high voltage power supplies, it is becoming common that the insulating materials face severe corona discharges. Corona discharge produces an eminently energized plasma of charged species and emits UV light. These plasma discharges emit charged particles on the surface of insulation and deteriorate the surface physically and chemically. The increase in temperature and humidity can accelerate the corona discharge intensity.

1.3 Physical properties of nanodielectric-based polyimide

For the last decade, the research has shown that when two materials in which one part is inorganic nanoparticles are combined to form a nanodielectric material, which

may have superior properties than single ones. The combined nanodielectric materials are known as polymer nanocomposites, when the base material is polymer matrix and the adding fillers are nanoparticles. Polymer nanocomposites have been used widely in academic research and industry [13]. The properties of nanocomposites change due to the large surface to volume ratio of the nanoparticles. The addition of nanoparticles into the base polymer matrix modifies the physical properties of composites. If the size of the nanoparticles is less than the critical length scale, then the physics of nanocomposite changes significantly. It has become one of the most reliable materials in electrical engineering since the first time the term nanocomposite was introduced in 1984 and since then it has been warmly accepted by the scientific community [13]. "Nanometric dielectrics," later named "Nanodielectrics" in 2004 by M.F. Frechette, is a nowadays popular term in the research community also known as nanocomposites made by the inclusion of nanometer size of nanoparticles in a polymeric matrix for dielectric applications [13]. In the beginning, the glass and ceramics were very common to use as solid dielectric materials. But, over time the power supplies demand increased abruptly, and these insulating materials were not enough to fulfill the demand. Therefore, new dielectric materials such as natural and synthetic polymers successfully overcome conventional dielectric materials. These new polymer-based dielectric materials have superior properties and lighter in weight to use in different applications.

1.3.1 Inorganic filling particles

Fillers are often fine-grained nanometer- or micrometer-sized particles and fibers, which can be made of organic or inorganic materials. Generally, such particles and fibers are named as conventional sized fillers according to their size range. Composites formed by using these fillers are labeled as conventional sized filled composites, for example, nanocomposites and microcomposites. Recently, filler materials have been used to improve electrical, mechanical strength, and thermal properties [5]. Polymers are chosen in electrical engineering according to the required application, and their properties can be modified by adding inorganic fillers in it. The quantity of fillers in the base polymer matrix is still under question from the literature that which amount by weight is most suitable to improve the desired properties. Therefore, we only use very low filler quantity of nanoparticles into the base polyimide. The common used organic polymers and their derived inorganic fillers are shown in **Table 2** [6].

Chemical family	Examples
Inorganics	
Oxides	Al_2O_3, SiO_2, MgO, ZnO, TiO_2, glass
Hydroxides	$Al(OH)_3$, $Mg(OH)_2$
Silicates	Talc, mica, nano clays, asbestos
Salts, compounds	$CaCO_3$, $BaSO_4$, $CaSO_4$, $BaTiO_3$, $SrTiO_3$
Metals	Al, Ag, Sn, Au, Cu
Nitrides, carbides	AlN, BN, Si_3N_4, SiC
Organics	
Carbon	Carbon fibers, carbon black, graphite fibers, carbon nanotubes
Natural polymers	Cellulose fibers, wood flour, flax
Synthetic polymers	Polyimide, polyester, polyethylene, polypropylene

Table 2.
Organic and inorganic fillers and their chemical family.

1.3.2 Particles' size, shape, and types

Various results of electrical, mechanical, and thermal properties have announced that the polymeric nanocomposites can be invaluable when a small amount of nanosize particles is appropriately chosen and dispersed into the base polymer matrix [14]. Composite material properties change dramatically due to the size, shape, and type of nanoscale particles. These nanoparticles have individual mechanical, electrical, and thermal properties [11]. Based on the size and type of particles, nanomaterials properties are shown in **Figure 3** and they are categorized as follows in **Figure 4** [15, 16].

1. Zero-dimensional (0-D)

2. One-dimensional (1-D)

3. Two-dimensional (2-D)

4. Three-dimensional (3-D)

If the number of the dimensions that are in the nano range is considered, exfoliated clay will be regarded as 0-D nanoparticles, because the diameter of these particles are in nanometer range. In order to utilize the ceramic nanoparticles in a better way with polymers, a potential studied has been done recently, especially in the field of the synthesis process and surface science. The most common studied ceramic nanoparticles are silica (silicon dioxide—SiO_2), alumina (Al_2O_3), titania (TiO_2), zirconia (ZnO), or silicon carbide (SiC).

1.3.3 Nanoparticle dispersion and distribution

The homogenous dispersion and distribution of nanoparticles are the major factor to improve nanocomposite dielectric material properties. A vital part of preparing
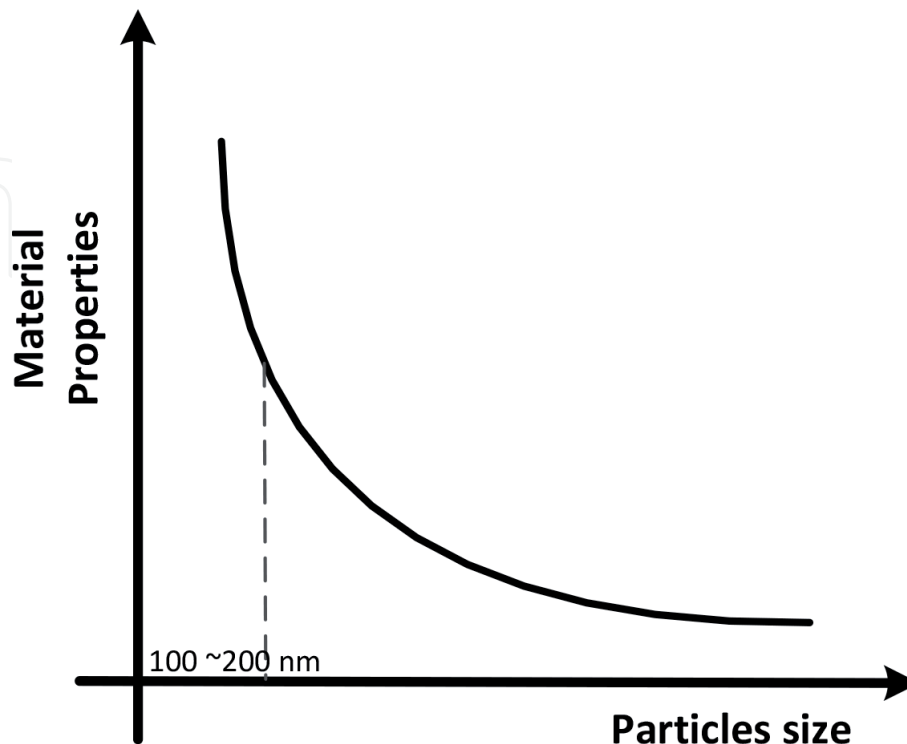

Figure 3.
Change in composite material properties with respect to particles' size.

1-D
Two dimensions (x, y) at nanoscale,
other dimension (L) is not

2-D
One dimensions (t) at nanoscale, other
two dimensions (Lx, Ly) are not

Lx

Ly

t ≤ 100

Nanowires, nanorods and nanotubes

Nanocoatings and nanofilms

(a)

(b)

0-D
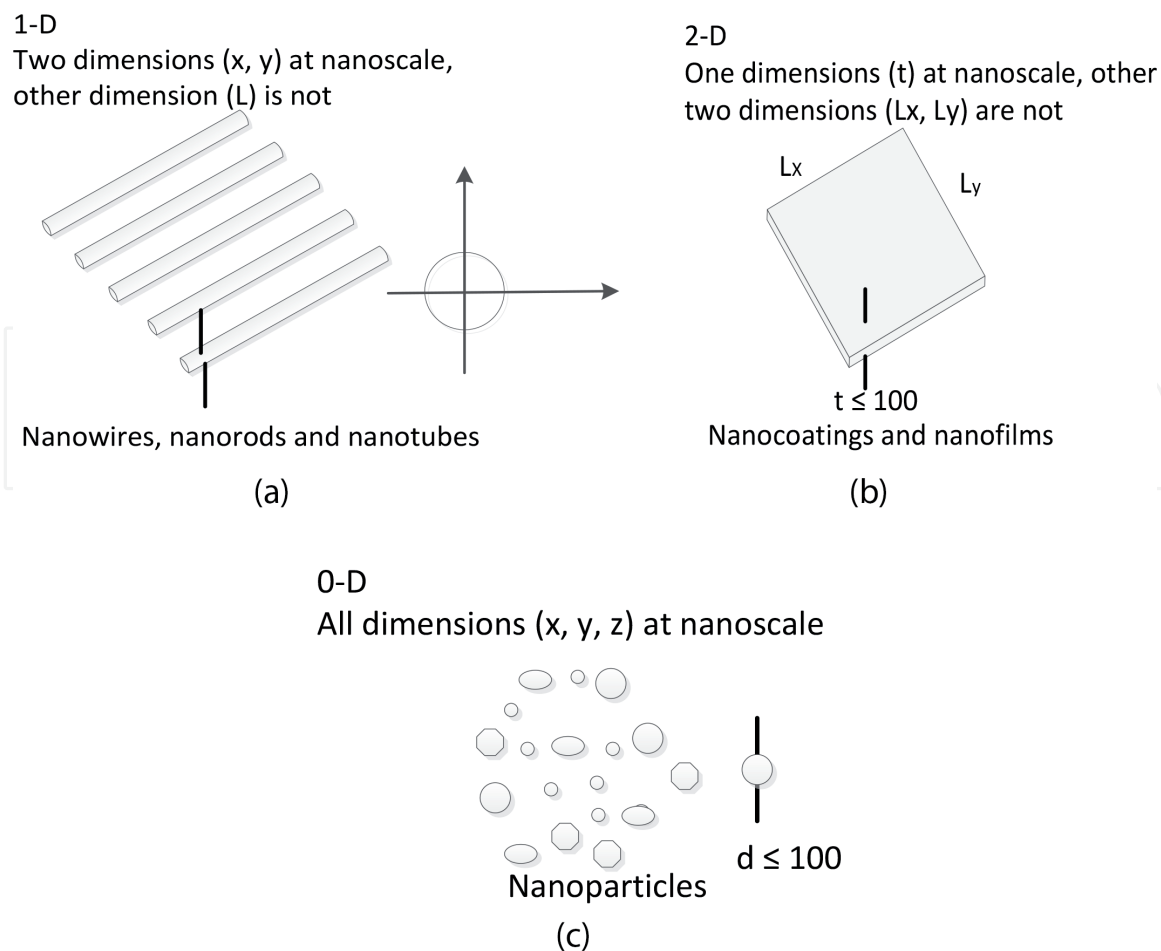All dimensions (x, y, z) at nanoscale

d ≤ 100

Nanoparticles

(c)

Figure 4.
Fillers' types, sizes, and shapes.

nanocomposites is the nanoparticle dispersion; they have heterogeneous surfaces, which cause variability in contact with the polyimide matrices. For better dispersion, several methods have been used such as the orientation of nanoparticles by applying an electric field, chemical treatment by using coupling agents, and plasma treatment. All these methods are adopted to solve the problems of heterogeneous agglomeration and the compatibility between the polyimide matrix and the nanoparticles. The nanoparticle mixing techniques such as mechanical milling, ultrasonication, high-speed stirrer, liquid dissolving, or heat melting can also affect the nanoparticle dispersion level. The size of particles and filler loading percentage can also influence the dispersion level [17]. Particles smaller than 80 nm tend to agglomerate and form more significant chunks of particles. The intermolecular forces keep nanoparticles together. The following particle parameters can influence the overall properties of polymer composites.

1. The size and shape of particles

2. The degree of particle dispersion

3. The surface modification of the particles

4. The particle-matrix interaction

1.3.4 Nanoparticles surface treatment

The interlinking of the PI and the nanoparticles depends on the functional groups and the surface energy of PI and nanoparticles. Some hydroxyl (OH)

functional groups can be formed on nanoparticles after surface modification, which provide a better interface and tightly bound with the PI matrix. To modify nanoparticle surface, different methods have been presented in recent papers such as deposition reaction modification, chemical surface treatment modification, high energy such as plasma source modification, and intercalation modification [14]. Affinity and polarity compatibility can also be used to create materials with homogenous dispersion of nanoparticles. For better interlink between the silica nanoparticles and the polyimide matrix, the surface of polar silica nanoparticles is modified using the KH550 coupling agent. Silica nanoparticles are hydrophilic, and polyimide is nonpolar, which is not compatible with mixing; therefore, the surface of the silica is modified to make it hydrophobic with hydroxyl (OH) functional groups on its surface, which are easy to bond with aromatic polyimide functional groups [14]. This surface modification is adopted to ensure success in the application. The interphase region around nanoparticles can be controlled using surface treatment [14].

1.3.5 Coupling agents

KH-550 silane coupling agent chemically known as 3-(2,3-epoxypropoxy) propyl trimethoxy silane is selected for silica nanoparticle surface modification. It contains an organic functional group, a linker, a silicon, and a hydroxyl group. The organic functional group can bond to the organic aromatic polyimide ring. The general chemical formula for the silane group and the hydrolyzable functional group, typically alkoxy, amine, or chlorine, involved in the reaction with the inorganic silica substrate. The silanol groups of the nanosilica surface can react with the hydroxyl groups of the silane after hydroxylation through hydrogen bonding. The covalent bond improves interfacial adhesion between inorganic silica particles and organic monomer molecules.

1.3.6 Plasma treatment

Nonthermal plasma technique is also prevalent these days to modify the surface of nanoparticles. This plasma technique enhances the compatibility between nanoparticles and polymer by modifying the interfacial area of nanoparticles. The plasma is produced by using a dielectric barrier discharge, which generates ions and reactive species high-energy electrons that interact with the surface of nanoparticles to modify their surface characteristics [14]. Therefore, higher surface reactivity and stronger interactions between the nanoparticles and the surrounding polymers can be acquired, comparing with traditional coupling agent modification.

2. Synthesis of polyimide

When one monomer reacts with other monomers, it forms a carbon chain of the polymer. In case of polyimide, the monomers such as diamine (ODA) react with another monomer such as dianhydride (PMDA) to form polyamic acid solution (PAA). In this reaction, an oxygen atom of diamine reacts with the hydrogen atom of dianhydride, and the hydrogen of dianhydride reacts with the carbon of diamine to give a repeated unit of polyamic acid. To obtain polyimide film, thermal heat is applied for several hours to evaporate DMAC solvent. The chemistry and the properties of polyimides can vary due to the availability of several monomers.
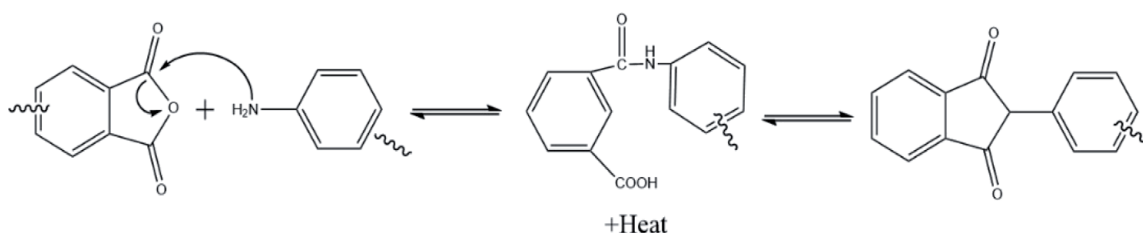
Figure 5.
Generalized reaction mechanism of aromatic imide formation.

The ratio of monomers can affect the molecular weight of PAA and change the molar mass of the final PI film [6, 18] (**Figure 5**).

2.1 Preparation mechanism for polyamic acid (PAA)

The aromatic PI film can only be synthesized from the solvent route using a two-step method. In the first step, PAA solution is synthesized using a reaction between dianhydride (pyromellitic dianhydride PMDA) and diamine (4,4'-oxydianiline ODA) at room temperature as shown in **Figure 6**. The dipolar aprotic solvents, such as N-methyl pyrrolidone (NMP) and N, N-dimethylacetamide (DMAc) are used to synthesize PAA solution. In the second step, PAA solution is converted into the final PI films after applying thermal imidization to evaporate solvent as explained in **Figure 7**. To make sure that PMDA did not absorb any moisture, it was heated for 2 h at 150°C. ODA was added into the beaker and mixed with DMAc for half an hour. Mechanical stirrer was used to stir the solution. PMDA was added into the solution in three parts, and the solution was further stirred for 24 h to get yellow color high molecular weight PAA solution as shown in **Figure 6**.

The reaction between the monomers to obtain viscous PAA solution is strongly dependent on the precise measurements. The following discussion will highlight important factors to select the monomers, solvents, and reaction conditions to get better results and avoid side reactions. The formation of the PAA solution may also involve some reversible reactions, which leads to the opening of the anhydride ring. Despite that, the forward rate of reaction is larger than the reverse rate depending on the purity of reagents. The molecular weight of the PAA product is also relying on the rate of difference between the forward and reverse reactions. Reverse reaction provokes when carboxyl group strikes to the adjacent polyacid group [6]. Some reagents can be used to stop the reverse reaction and provokes a forward reaction. The amino group basicity and PMDA electrophilicity in different solvents can change the equilibrium constant, and the reaction is exothermic; therefore, it should carry out at room temperature to minimize the equilibrium constant effect.
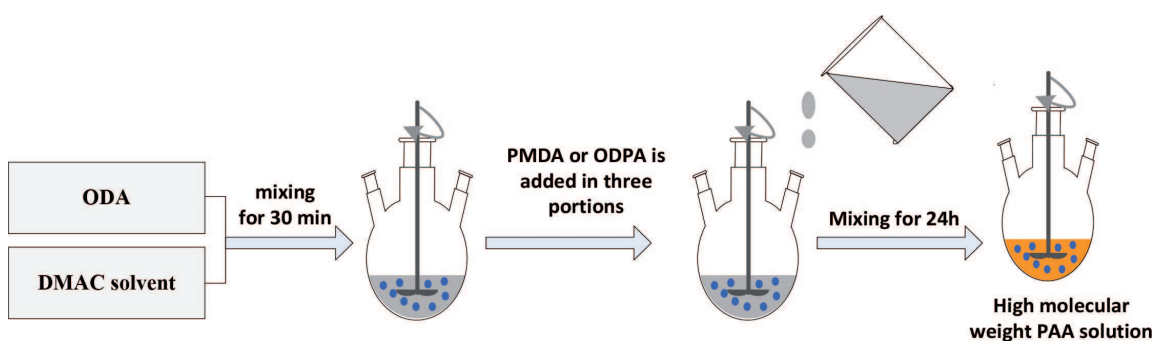

Figure 6.
Synthesis process of PAA solution.

2.2 Monomer reactivity conditions

As explained in the above section, the PAA solution is formed by nucleophilic substitution of carbon atom in carbonyl group of the dianhydride with a diamine. Therefore, electrophilicity of carbonyl group carbon atom and nucleophilicity of amino group nitrogen atom can be controlled using electron affinity measurement of both dianhydride and diamine. PMDA has the highest electron affinity and shows strong reactivity with diamines compared with other dianhydrides such as DSDA, BTDA, BPDA, and ODPA. The change in the structure of the diamines and dianhydride can affect the reaction significantly. These highest electron affinity dianhydrides can easily absorb moisture; therefore, they must keep moisture-free environment.

2.3 Factors involved in the molecular weight of PAA

The following factors are required to increase or decrease the molecular weight of PAA:

1. A slight increase in dianhydride quantity and the addition of solid dianhydride into the diamine solution can increase the molecular weight of PAA.

2. The order of the addition of the monomers, the solid mode of dianhydride addition into diamine solution, can avoid an immediate reaction and minimize the side reactions with water and impurities.

3. Minimize the side reactions to avoid dianhydride reaction with water and impurities.

4. Lesser quantity of solvent will help to reduce the impurities and water contents and increase the concentration of the monomer.

5. Storage of PAA solution for a long time can decrease the molecular weight. It can be due to the initiative of the hydrolysis process and chemical breakdown of a compound, and the other reason for this low viscosity can be the reverse reaction.

6. The solvents can also slightly affect molecular weight. The universal solvents are DMF, DMAC, and NMP, and the reaction is exothermic in which monomers are basic aromatic amines and protic anhydrides, and the final product is an acid. Therefore, the strong rate of the reaction is expected for more basic and more polar solvents.

2.4 Synthesis of PAA/nanoparticle composite solution

The PAA/SiO_2 nanocomposite solution was synthesized by applying the in-situ polymerization method, as elaborated in **Figure 7**. For the better link between PI and nanoparticles, SiO_2 was treated with a KH-550 coupling agent to modify its surface. Altered surface SiO_2 nanoparticles and dimethylacetamide (DMAC) were dispersed by applying ultrasonication and high-speed stirring, then oxy dianiline (ODA) was added into the solution and mixed for 1 h. After that pyromellitic dianhydride (PMDA) was added into two portions. For the first portion, almost 90% PMDA was added and mixed for 30 min, then the remaining 10% PMDA was added and mixed for 2–6 h until yellowish color high molecular weight PAA solution was obtained.
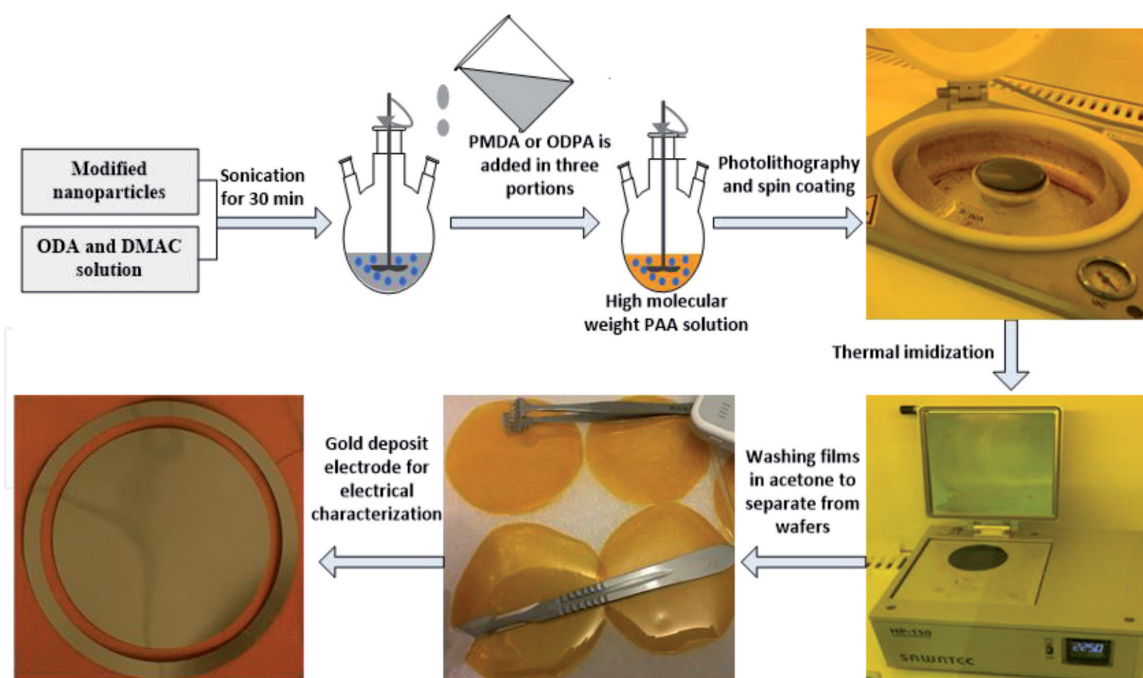
Figure 7.
Polyimide film synthesis process.

2.5 PI film casting using glass and brass substrate

Higher molecular weight polyamic acid solution dissolved in dimethylacetamide-based solvents is suitable for PI film casting using a variety of substrates, for example, teflon, alumina, glass, silicon wafers, brass, and copper. After coating the polyamic solution on the substrate, the precursor is thermally cured into an aromatic polyimide film. Both static and dynamic casting techniques can be used depending on the final product size and available tooling. In static casting, glass was used as a substrate to cast the PAA solution on it using a glass rod. Typically, this technique is easy, but it requires more material per substrate and difficult to control the thickness of PI films.

2.6 Casting PI films using a spin coating technique

Spin coating is the most prevalent technique to deposit PAA solution onto substrates such as silicon wafers and brass. The dynamic deposition technique uses less material, but it requires precision to control the operation. While depositing, it is important to pour PAA solution in the center of the wafer. Generally, we can achieve the maximum speed up to 6000 rpm, if the vacuum chunk has enough suction to hold the substrate while depositing PAA solution onto the surface of substrates. The PAA solution was homogenously distributed over the silicon wafer substrates during spinning. The acceleration of speed was programmed to start with low speed, slowly rise to maximum speed, and finally decrease the speed slowly to allow the coating flow across the substrate edges homogenously. Several spin speed steps can be used to control the flow of solution to cover more than 80% of the substrate before achieving the final speed.

2.7 Casting PI and nanocomposite/PI multilayer films

PI is obtained using the curing method in which a solvent is evaporated with the increase of temperature. During the PI film curing process from the polyamic acid (PAA) solution, there is a strong tendency of nanoparticles to get agglomerated. They may float on the surface or decant. Both effects can increase the chances

of agglomeration and may influence the interface thickness and permittivity of samples and result in lower dielectric properties of PI films. Keeping this in mind, we prepared a multilayer (two and three layers) structure in which the top layer consists of a very thin PI/SiO$_2$ nanocomposite (NPI) layer, and the bottom is composed of pure PI layer [4]. By doing this, we are giving less space for nanoparticles to get agglomerated. In order to cast the PI/nanocomposite multilayer films, two different spin speeds were used for a two-layer structure. After calibrating the right speed to get right thickness, we select 20 s at speed of 500 rpm to get around 60 μm thick first base layer of PI film and soft bake for 30 min at 60 and 100°C temperature, then we use 30 s of 1000 rpm to get second nanocomposite/PI 20 μm thick layer.

2.8 Controlling the thickness

The thickness of the casted PI film depends on several factors such as the viscosity, molecular weight of the PAA solution, and the spin speed of spin coater. Varying PI film thickness in the range of 10–150 μm can be achieved by using a spin coating method. Two different viscosity solutions of PAA are used to obtain PI films as shown in **Figure 8**. The film thickness decreases with increasing spin rate. To avoid the bubbles and the accumulation of excessive blocks of PAA solution, spin cycle time should increase because prolonger spin times improve film coating uniformity, but at the same time, it can reduce the film thickness.

2.9 Thermal imidization of a polyamic acid (PAA)

The PI films can be cured of the PAA solution after applying thermal imidization. After casting the PAA solution onto the substrate, thermal steps with temperature from 100 to 350°C were used to evaporate the solvents. According to the literature, various thermal steps and different temperature ranges have been utilized to achieve 100% imidization from PAA to PI. Two main thermal imidization ways are as follows:

1. Baking films with slowly increasing in temperature up to 350°C according to the flexibility and T$_g$ of the PI film.
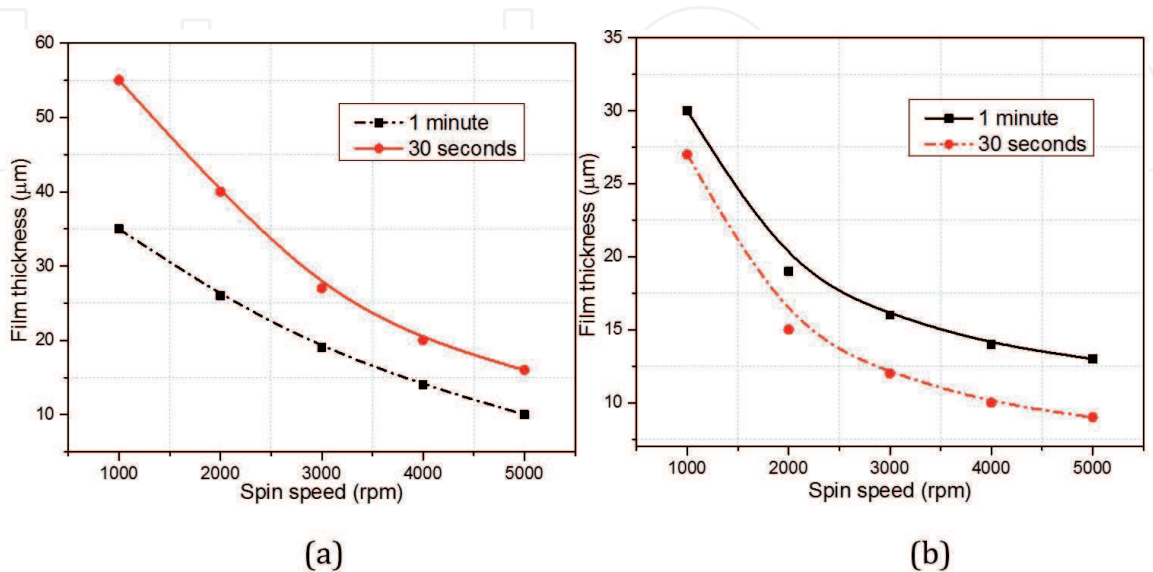

(a) (b)

Figure 8.
Film thickness variation at different spin coater speeds (a) PAA solution high molecular weight and (b) PAA solution slight less molecular weight.

2. Start baking PAA with the temperature 100°C for 1 h, then baking at 200°C for 1 hour, then baking at 300°C and keeping for 1 h and slowly cool down to room temperature.

Several arduous factors are involved in the above simple-looking thermal imidization process to predispose the degree of imidization of PI films. During imidization, the remaining solvent at the later stages determines the stability of PI films. In early stages, the imidization process is faster, and several dynamic changing in physical properties happen due to the basicity of the amide solvent to accept protons and the amicable conformation of the amic acid to increase the mobility of the reacting functional groups [6]. At later stages, the rate of imidization slows down due to the decyclohydration of the open amic acid group into the closed imide ring, which decreases the chain mobility, and the T_g approaches the reaction temperature [6].

2.10 Determination of the degree of imidization using FTIR

When one monomer reacts with other monomer, it forms a carbon chain of the polymer. In our case, a single unit of two monomers such as diamine (ODA) and dianhydride (PMDA) reacts with each other to form a single unit of polyamic acid (PAA) solution. In this reaction, an oxygen atom of diamine reacts with the hydrogen atom of dianhydride, and the hydrogen atom of dianhydride reacts with the carbon atom of diamine to give us a repeated unit of PAA. After obtaining PAA, thermal imidization was applied to cure PI and PI/ SiO_2 films.

Fourier transform infrared spectroscopy (FTIR) is a promising tool to determine the degree of imidization despite a minor error in measurement due to its sensitivity to chemical change. The bond composition of PI atomic structure was studied by FTIR spectroscopy to analyze the chemical bonds present in PI. The bands most frequently utilized are imide absorption bands near 1780 cm^{-1} (C=O asymmetrical stretching), 1380 cm^{-1} (C—N stretching), and 725 cm^{-1} (C=O bending). This study describes the chemical characterization of half cured and fully cured PI and PI/SiO_2 films. The range of wavelength used was from 650 to 4000 cm^{-1}. The PI subatomic structure is composed of a molecular chain containing the functional groups such as aromatic rings, amide rings, and some noncyclic ether rings. These functional groups have discrete chemical bonds such as C—N—C, C=O, benzene (C_6H_n), ether link (C—O—C), and —OCH_2—CH_2 deformation. The functional groups of PI polymer chains provide the level of linkage with subatoms as well as the linkage with silicon oxide nanoparticles. Imide group contains imide carbonyl in-phase and out-of-phase stretching, the C—N—C axial, transverse, and out-of-phase stretching. The absorbance peaks at 1371, 1112, and 721 cm^{-1} indicate the transverse and axial stretching of C—N—C bond, and the reasons of 1781 and 1720 cm^{-1} peaks are in-phase and out-of-phase stretching of C=O in imide ring. Aromatic ring is divided into tangential, radial skeletal, and out-of-plane vibrations. The peak at 1590 cm^{-1} relates to tangential C—C vibrations. The peak at 1280 cm^{-1} is tangential phenyl ring vibrations. The other 1480, 1168, 1087, 1011, 843, and 788 cm^{-1} peaks describe about the tangential, radial skeletal, and out-of-plane bending vibrations of C_6H_n in aromatic ring. The peaks at 1234 and 1454 cm^{-1} relate to the bond of ether link (C—O—C), and 1416 cm^{-1} peak corresponds to —OCH_2—CH_2 deformation. **Figure 9(a)** and **(b)** shows the FTIR spectra of changes in the bonds of half cured and fully cured PI films at different temperatures and time to determine the degree of imidization to obtain imide ring.
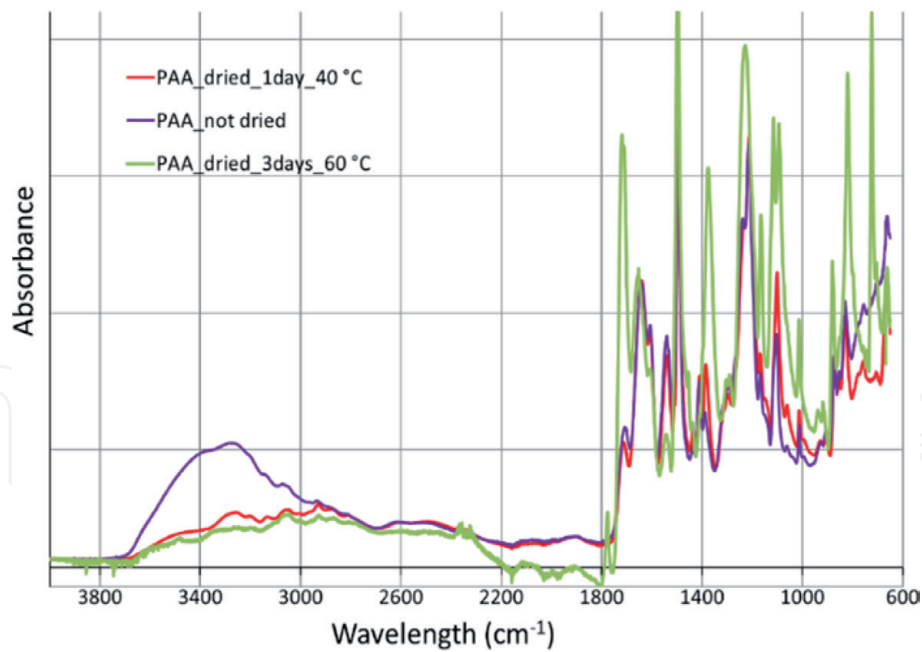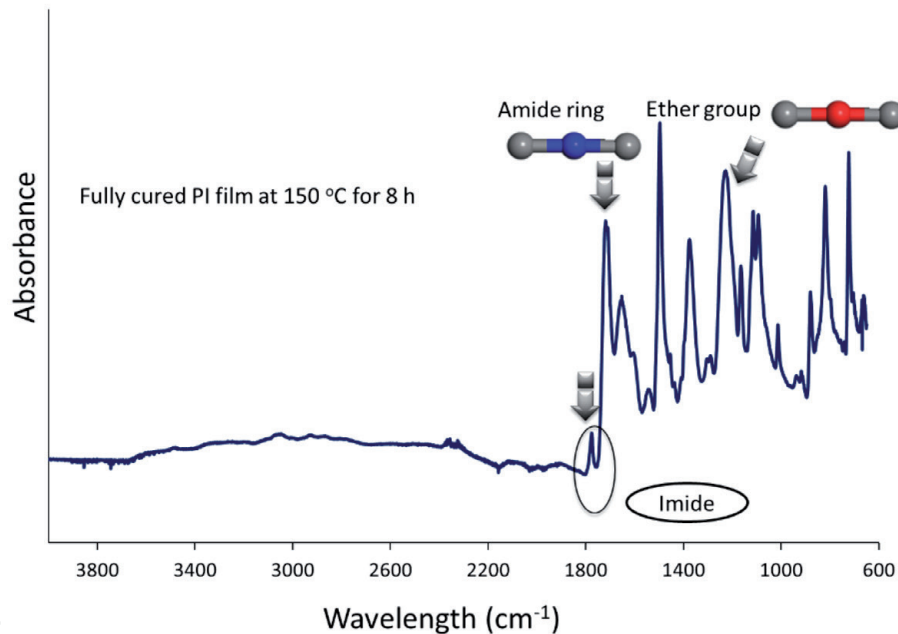
Figure 9.
(a) Half cured PI film at different temperature and time and (b) zoom version of main function group peaks.

In fully cured PI films, as shown from **Figure 9**, the bonds are grouped into amide rings, aromatic rings, and noncyclical stretching based on atom vibrations [18]. The intensity of the absorption band at 3463 cm^{-1} corresponding to the stretch vibration of −OH bond.

3. Dielectric properties of PI/nanocomposites and their modeling

To simulate the electrical field distribution in PI/nanocomposites, COMSOL-MATLAB Live link and image processing tools were used to build the PI/SIO₂ (NPI) 3D model. The boundary conditions and geometry of the model were obtained from TEM/SEM images of laboratory-produced samples, as shown in
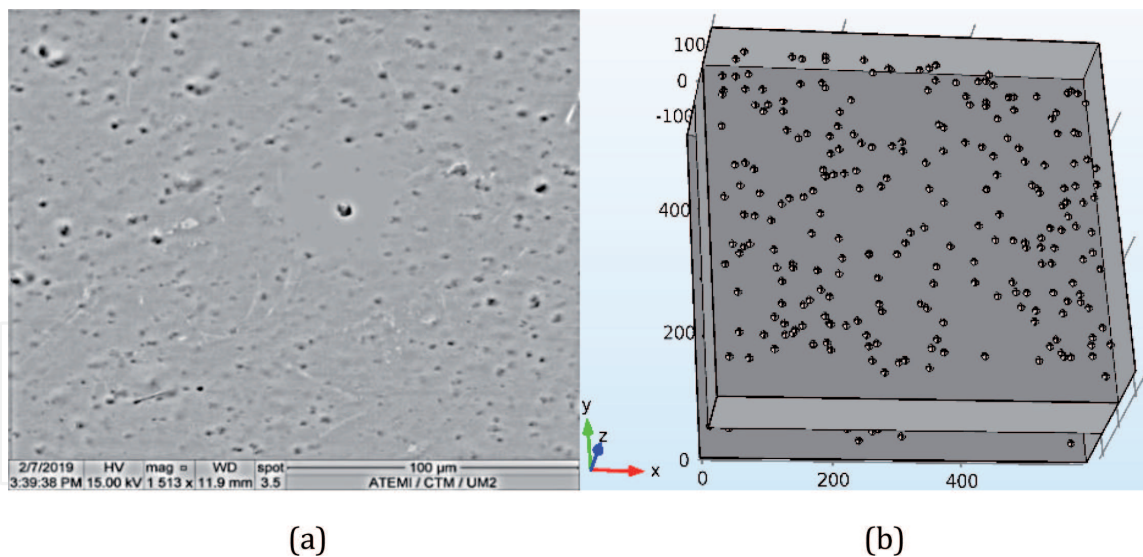
Figure 10.
(a) TEM image of PI/SiO₂ and (b) model in COMSOL using MATLAB Live Link.

Figure 10a, and its respectfully constructed model, as shown in **Figure 10b**. The positions of nanoparticle coordinates (x, y) in the model were taken from TEM/SEM images after converting the image into binary. For z-axis information, there are two possible ways to estimate the z-axis parameter. Either we can assume color intensity level from SEM/TEM images of **Figure 10a** as the depth (z-axis) of nanoparticles to construct 3D model or we can use SEM cross-sectional view information (if particle size is viewable from SEM/TEM) to find the depth of nanoparticles inside the bulk of samples to build model. For our samples, we have used the color intensity technique to obtain the z-axis parameter and create a 3D model. To construct the model, we picked a clear TEM/SEM image, applied an image processing to remove background noise, and finally converted it into the binary. To select the required data from the binary image, we adjusted the image to binary conversion threshold, nanoparticles size, and circularity level. The data contained different information about the particle size and shape (x, y) coordinates. The z-axis related to the depth of each particle is obtained using a small code in MATLAB according to the intensity level of each particle. In this simulation model, the dielectric permittivity of the PI matrix is taken to be $\varepsilon_1 = 3.4$, and that of the silica nanoparticles is $\varepsilon_2 = 3.6$. The nanoparticles were assumed to have a spherical shape of 10 nm radiuses calculated after image processing. The top surface of the 3D model was applied by the constant electric potential of ($V = 10$ V), and the bottom surface was grounded to 0 V. The volume fraction of nanoparticles is constant and set at 1% for single and multilayer insulation structures. The details to construct the model are presented in **Figure 11**.

After constructing the continuum model in COMSOL, the finite element method (FEM) was utilized to observe the nonlinear electric field distribution, as shown in **Figure 12**. The nanodielectric modeling with FEM can be used to predict its dielectric strength based on electric field distribution. FEM was used to calculate the electric field enhancement factor and polarization charge density, as shown in **Figure 13a** and **b**, respectively. Single and multilayers of PI/silica nanocomposite models were simulated with altered nanoparticle permittivity and position. The analysis is focused on calculating the peak electric field enhancement factor (peak EFEF) in the sample from Eq. (3).

$$\text{Peak EFEF} = \frac{\text{maximum electricfield (kV/mm)}}{\text{applied electric field (kV/mm)}} \tag{3}$$
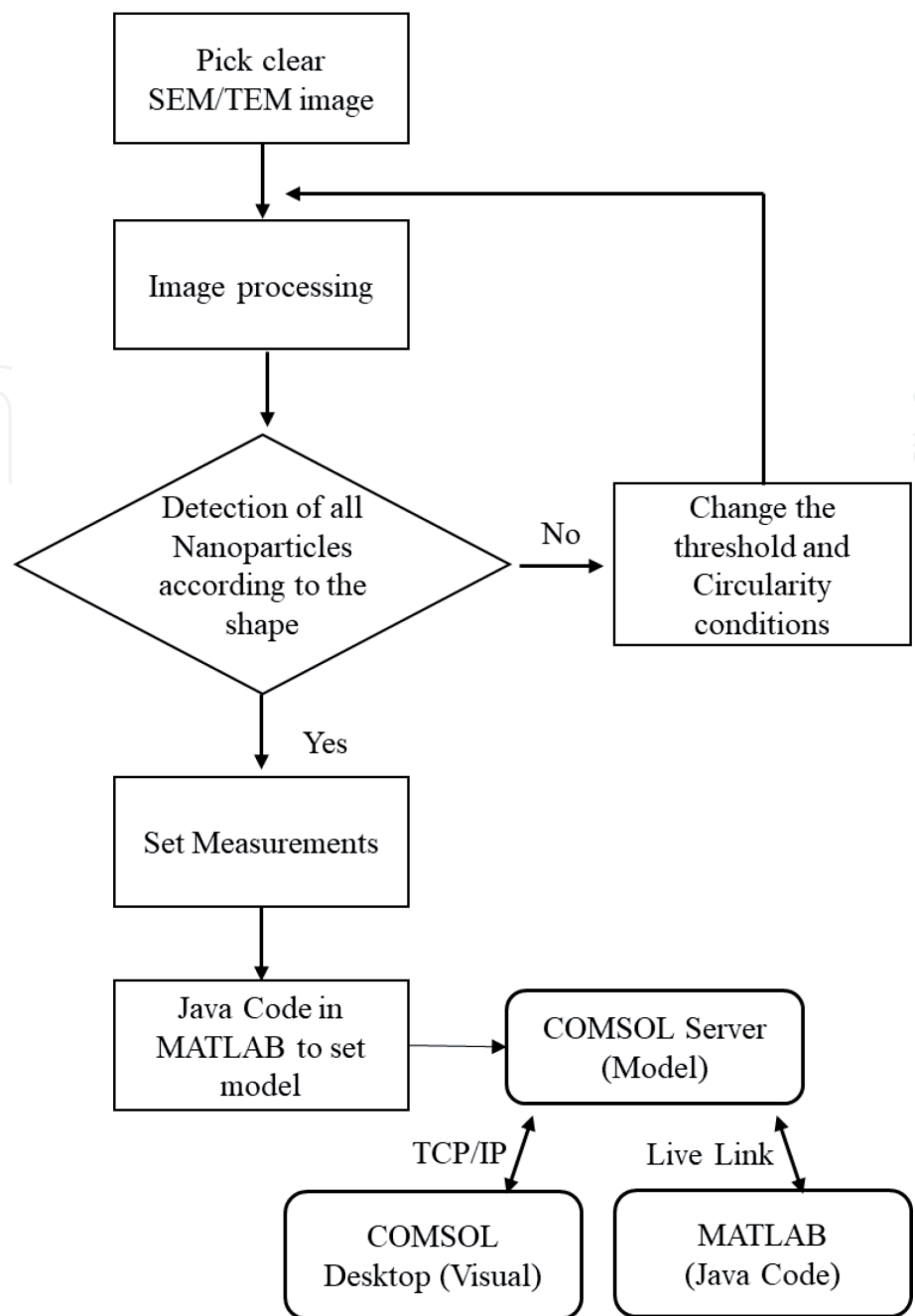
Figure 11.
Model building algorithm.

The simulation results from **Figure 13** show that the electric field enhancement factor (EFEF) and polarization charge density vary with the increase in nanoparticle permittivity, and lesser EFEF is observed in three-layer PI films compared with single-layer models such as top agglomeration and bottom agglomeration. As shown in the simulation solution of **Figure 12**, the maximum electric field exists at the surface between the nanoparticles and the PI matrix in the direction of the z-axis, while the linear electric field is observed in the remaining area of PI/nanocomposite model.

The uniform dispersion of nanoparticle models improved the electric field distribution and reduced the electric field localization as happened in single-layer agglomerated models. The highest electric field and polarization density were obtained in a single-layer top agglomeration model. One of the main reasons for this enhancement can be the change in equivalence capacitance of the sample due to the agglomeration of the nanoparticles, which influence the effective permittivity of the overall sample. The electric field is also influenced due to the shape of the outer surface of nanoparticles because if agglomeration happens, there is a chance that the
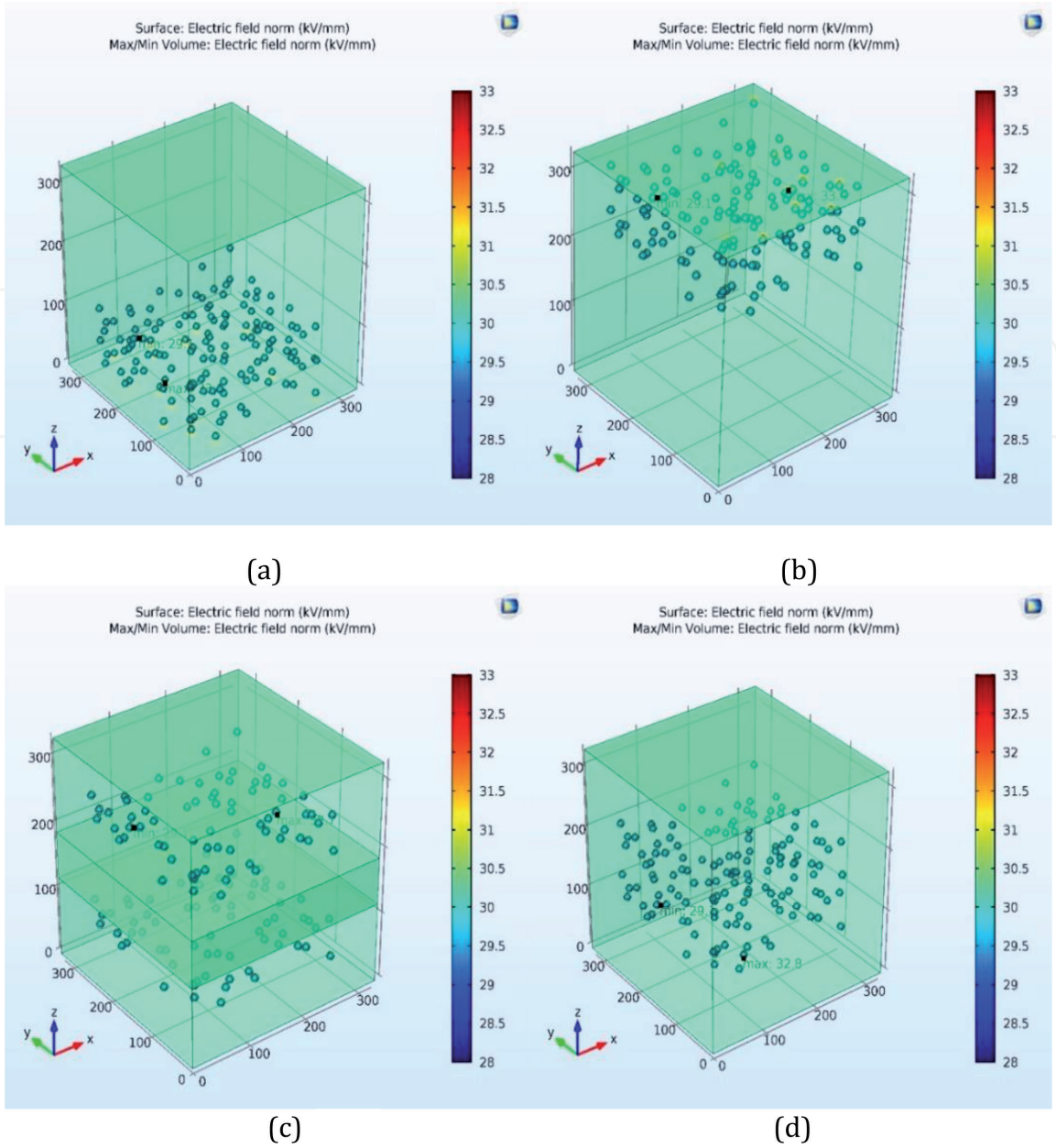
Figure 12.
(a) Top agglomeration, (b) bottom agglomeration, (c) three-layer homogenous dispersion, and (d) three-layer original homogenous distribution.
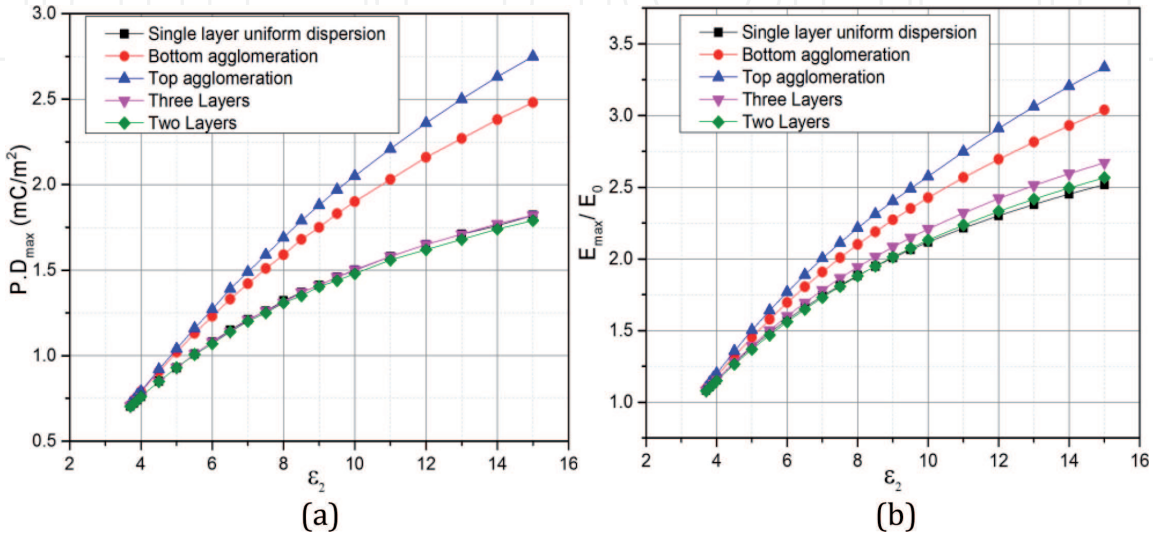

Figure 13.
Calculation of (a) electric field enhancement factor and (b) polarization charge density.

combined particles may change the circularity level and transform the shape into the sharp edges, which increase the local electric field around those edges. Another reason for higher EFEF in agglomeration models can be due to a decrease in the interparticle distance.

To verify the simulation results, electrical characterizations such as the space charge are also determined through the experimental results for single and

(a)

(b)
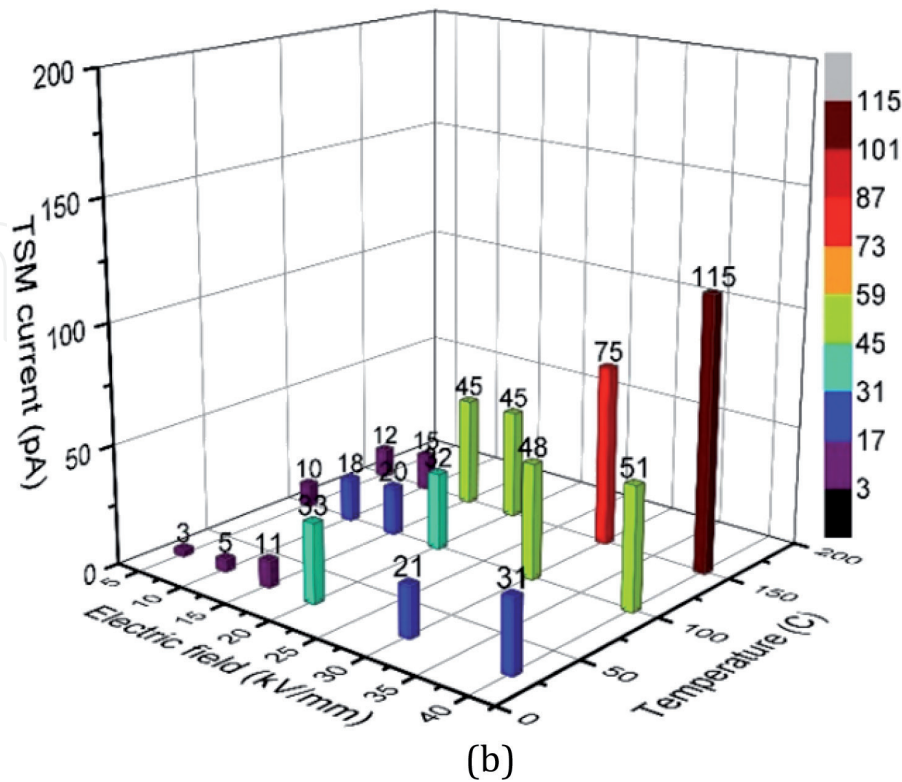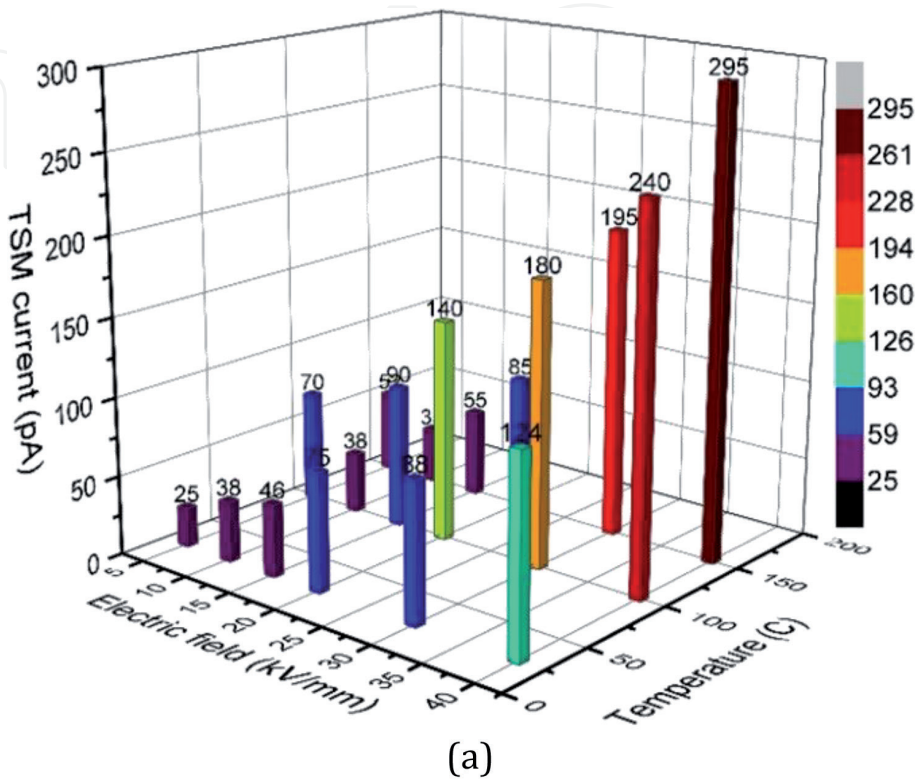
Figure 14.
TS current after applying different temperatures and electric fields: (a) single-layer NPI samples and (b) two-layer PI-NPI samples.

multilayer PI nanocomposite films [19]. For space charge measurements, the experiments are conducted using the thermal step method (TSM) to detect the capacity of these new insulating materials to accumulate/release space charges after thermoelectric poling, close to the practical applications. An electric field between 5 and 40 kV/mm is applied at 50, 100, and 150°C for 1 h [19]. The results presented in **Figure 14(a)** for single-layer NPI films and **Figure 14(b)** for double-layer PI-NPI films illustrate that the amplitude of the TSM current acquired for double-layer PI-NPI films is lesser than the single-layer NPI films at all electric fields and temperature conditions. The lower amplitude of TSM current is due to a lower level of space charge accumulation. Moreover, two opposite TSM current signs correspond to different dominant charges. The current sign changes from positive to negative from low temperature 50°C to higher temperature 150°C, especially for single-layer NPI samples. The sign of current corresponds to the same dominant charge injected from the electrode and shows an increase in accumulated space charge when the poling applied field increases. A thin layer of NPI on PI samples highlights lower TSM currents, and this behavior is more visible at higher electric fields because the signal-to-noise ratio is improved at the higher electric field. Thus, the coating of thin NPI on PI acts as a barrier and reduces the charge injection from electrodes. These coated layers are discharged resistive and increase the charge dissipation rate to reduce the space charge accumulation. Adding nanoparticles in the form of multistructure improves its dispersion by reducing the layer thickness and therefore leads to better dielectric properties, as presented in results.

4. Conclusions

A brief introduction of the physical properties of PI films and their derived nanoparticles was described in this chapter. The preparation of PI nanocomposite is a complex process with many variables involved. Several methods were probed before an optimal synthesis process was found. A detailed synthesis process optimization of multilayer PI nanocomposite films is described in this chapter to understand all variables, which can influence the dielectric properties of the final product. The polyimide/nanocomposite multilayer 3D model based on actual boundary conditions from SEM images of synthesized samples is also constructed and simulated in COMSOL multiphysics software. Effect of nanoparticle agglomeration in microstructures, with the impact of nanoparticle dispersion on the electric field enhancement, is explicitly described in this model. The dielectric properties such as space charge using thermal step method (TSM) technique were also measured to compare simulation results. Our results demonstrate that the chances of nanoparticle agglomeration are reduced by using a thin layer of PI/nanocomposite on PI film instead of using one single layer of PI/nanocomposite film. In consequence, less space charge and low electrical fields are observed in multilayer films. Our methods will help to reliably predict the dielectric strength of polymer/nanocomposite insulating materials. Additionally, the new synthesized multilayer PI/nanocomposite insulating material will ensure reliable operation for electric motors and increase its lifespan.

Acknowledgements

Conflict of interest

The book chapter was written with the contributions of all authors. All authors have approved the final version of the chapter. The authors declare no competing financial interest.

Author details

Shakeel Akram[1*], Jérôme Castellon[1*], Serge Agnel[1] and Jean-Pierre Habas[2]

1 Institut d'Electronique et des Systèmes (IES), CNRS, University of Montpellier, Montpellier, France

2 Institut Charles Gerhardt de Montpellier (ICGM), CNRS, Equipe Ingénierie et Architectures Macromoléculaires, University of Montpellier, Montpellier, France

*Address all correspondence to: akram@ies.univ-montp2.fr
and jerome.castellon@umontpellier.fr

IntechOpen

References

[1] Yang Y, Jinliang H, Guangning W, Jun H. Thermal stabilization effect of Al_2O_3 nano-dopants improves the high-temperature dielectric performance of polyimide. Scientific Reports. 2015;**5**:16986. DOI: 10.1038/srep16986

[2] Shakeel A, Yang Y, Zhong X, Bhutta S, Wu G, Castellon J, et al. Influence of nano layer structure of polyimide film on space charge behavior and trap levels. IEEE Transactions on Dielectrics and Electrical Insulation. 2018;**25**:146-469. DOI: 10.1109/TDEI.2018.007506

[3] Diaham S, Zelmat S, Locatelli ML, Dinculescu S, Decup M, Lebey T. Dielectric breakdown of polyimide films: Area, thickness and temperature dependence. IEEE Transactions on Dielectrics and Electrical Insulation. 2010;**17**:18-27. DOI: 10.1109/TDEI.2010.5411997

[4] Akram S, Castellon J, Agnel S, Khan MZ. Space charge analysis of multi-structure polyimide films using TSM. In: Proceedings of the IEEE International Conference on Electrical Insulation and Dielectric Phenomena (CEIDP '18); 21-24 October 2018; Cancun. Mexico: IEEE; 2018. pp. 34-37

[5] Andritsch T, Fabiani D, Vazquez IR. Nanodielectrics—Examples of preparation and microstructure. IEEE Electrical Insulation Magazine. 2013;**29**:21-28. DOI: 10.1109/MEI.2013.6648750

[6] Debra LD. Synthesis and characterization of thermosetting polyimide oligomers for microelectronics packing [thesis]. Blacksburg Virginia: Virginia Polytechnic Institute and State University; 2000

[7] Simpson JO, Clair AK. Fundamental insight on developing low dielectric constant polyimides. Thin Solid Films. 1997;**308-309**:480-485. DOI: 10.1016/S0040-6090(97)00481-1

[8] Luo Y, Wu G, Liu J, Peng J, Zhu G, Guoqiang G. Investigation of temperature effects on voltage endurance for polyimide/Al_2O_3 nanodielectrics. IEEE Transactions on Dielectrics and Electrical Insulation. 2014;**21**:1824-1834. DOI: 10.1109/TDEI.2014.004305

[9] Jonscher AK. Dielectric relaxation in solids. Journal of Physics D: Applied Physics. 1999;**32**:57-70. DOI: 10.1088/0022-3727/32/14/201

[10] Shakeel A, Wu G, GuoQiang G, Liu Y. Cavity and interface effect of PI-film on charge accumulation and PD activity under bipolar pulse voltage. Journal of Electrical Engineering and Technology. 2015;**10**:2089-2098. DOI: 10.5370/JEET.2015.10.5.2089

[11] Hafiz ZA, Murat K. The changes in electrical and interfacial properties of polyimide exposed to dielectric barrier bischarge in SF6 medium. The Scientific World Journal. 2013;**2013**:1-7. DOI: 10.1155/2013/890454

[12] Starr W. Polymeric outdoor insulation. IEEE Transactions on Electrical Insulation. 1990;**25**:125-136. DOI: 10.1109/14.64507

[13] Frechette MF, Trudeau ML, Alamdar HD, Boily S. Introductory remarks on nanodielectrics. IEEE Transactions on Dielectrics and Electrical Insulation. 2004;**11**:808-818. DOI: 10.1109/TDEI.2004.1349786

[14] Nelson JK. Dielectric Polymer Nanocomposites. Springer; 2010. pp. 31-45. DOI: 10.1007/978-1-4419-1591-7

[15] Roman K. Thermal and electrical properties of nanocomposites,

including material properties [Thesis]. Astrophysical Journal Letters. 2012

[16] Mai Y-W, Yu Z-Z. Polymer Nanocomposites. Woodhead Publishing Ltd. [Book]; 2006

[17] Gaurav M, Suprakas Sinha R, Shofner ML, Shanfeng W, Jin Z. Polymer nanocomposites Processing, characterization, and applications. Journal of Nanomaterials. 2013;**2014**:403492. DOI: 10.1155/2014/403492

[18] Shakeel A, Guoqiang G, Yang L, Jian Z, Wu G. Degradation mechanism of $A1_2O_3$ nano filled polyimide film due to surface discharge under square impulse voltage. IEEE Transactions on Dielectrics and Electrical Insulation. 2015;**22**:3341-3349. DOI: 10.1109/TDEI.2015.005059

[19] Shakeel A, Jérôme C, Serge A, Jean-Pierre H, Zhou K, Tariq Nazir M. Impact of nanocomposite thin layer on nanoparticles dispersion and their dielectric properties. In: Proceedings of the IEEE International Conference on Electrical Insulation and Dielectric Phenomena (CEIDP '19); 20-23 October. Vol. 2019. Richland, Washington. USA: IEEE; 2019. pp. 381-384